NIH Public Access
Author Manuscript
Proteomics Clin Appl. Author manuscript; available in PMC 2011 December 20.

Published in final edited form as:
Proteomics Clin Appl. 2010 March ; 4(3): 295–303. doi:10.1002/prca.200900083.

Biomarkers of neurological status in HIV infection: A three year study

Ann B. Ragin, PhD[a], **Ying Wu, MD**[b], **Renee Ochs, BA**[a], **Rachel Scheidegger, BA**[c], **Bruce A. Cohen, MD**[d], **Robert R. Edelman, MD**[b], **Leon G. Epstein, MD**[e], and **Justin McArthur, MBBS, MPH**[f]

[a]Dept. of Radiology, Northwestern University, Chicago, IL, USA

[b]Center for Advanced Imaging, North Shore University Hospital, Evanston, IL, USA

[c]Harvard-MIT Division of Health Sciences & Technology, Cambridge, MA, USA

[d]Dept. of Neurology, Northwestern University, Chicago, Illinois, USA

[e]Division of Neurology, Children's Memorial Hospital, Chicago, IL, USA

[f]Dept. of Neurology, Johns Hopkins University, Baltimore, MD, USA

Abstract

In this investigation, circulating cytokines and chemokines were screened as correlates of brain injury in individuals with advanced Human Immunodeficiency Virus (HIV) infection. Markers were quantified using high throughput multiplexed analysis at baseline and three years later in the clinical course. Neurological status was ascertained based on objective measurements of the brain derived *in vivo* with Magnetic Resonance (MR) segmentation algorithms and with Diffusion Tensor Imaging (DTI). Of the markers examined, Monocyte Chemoattractant Protein-1 (n.b. MCP-1 or CCL-2) was the most prominent correlate of brain injury. At the initial assessment, elevated MCP-1 levels correlated with alterations in brain white matter. The relationship to brain injury was more extensive three years later; MCP-1 was significantly correlated with both microstructural measures (fractional anisotropy and mean diffusivity) and with brain atrophy (in gray matter and overall parenchyma).

Conclusion—These findings provide further evidence of the potential importance of MCP-1 as a marker of neurological injury in HIV infection. These observations build on our prior descriptions suggesting that elevated levels of MCP-1 may be a useful predictive marker for HIV-associated neurocognitive disorder (HAND). As a potent chemoattractant, MCP-1 may mediate injury through participation in self-reinforcing cycles of chronic immune activation and cytokine/chemokine-mediated neurotoxicity.

Keywords

Brain Volumetry; Diffusion Tensor Imaging; HIV-Neurological Disease; MCP-1; Proteomics

Correspondence: Ann B. Ragin, PhD, Department of Radiology, Feinberg School of Medicine; Northwestern University, 737 N. Michigan Avenue Suite 1600, Chicago IL 60611 FAX: 312-926-5991; ann-ragin@northwestern.edu).

Conflicts of Interest: None. The authors had full access to all the study data and final responsibility for the decision to submit for publication.

NIH-PA Author Manuscript
NIH-PA Author Manuscript
NIH-PA Author Manuscript

NIH-PA Author Manuscript
NIH-PA Author Manuscript
NIH-PA Author Manuscript

1. Introduction

Advances in the treatment of HIV infection have enhanced virological control and increased the survival duration of infected individuals. Nevertheless, the risk of cognitive deterioration from brain injury is considerable [1-4], and HAND remains a prevalent condition despite relatively widespread use of potent antiretrovirals. HIV Encephalitis, the pathologic correlate of dementia, is evident in many infected individuals at autopsy [5]. *In vivo* brain imaging studies demonstrate thinning of the cerebral cortex, generalized atrophy and other evidence of injury, for a review, see [6]. Factors underlying increased vulnerability or resistance to these neuropathological changes, however, have been difficult to determine. Ongoing brain injury may be subclinical for long periods or characterized by a fluctuating presentation. While several candidate markers have been proposed [7], there are currently no well-validated laboratory indicators of HIV neurological progression [2]. Furthermore, established markers of systemic HIV disease progression, such as CD4 absolute cell count and viral replication measured in the peripheral circulation (HIV RNA), may not correspond to changes occurring in viral reservoirs or privileged anatomic compartments, such as the brain and bone marrow.

Multiplexed analytic capabilities promise to accelerate identification of molecular biomarkers associated with clinical outcome. With Luminex-based high throughput bulk assay, a large number of bioassays can be performed simultaneously from a single biological specimen. Noninvasive Magnetic Resonance (MR) imaging technologies are also available that can be used to generate objective measurements of the brain *in vivo*, thereby overcoming the difficulty determining the degree of neurological involvement in individual subjects. This investigation combined proteomic and quantitative brain imaging technologies. Objective measurements of the brain were determined in individuals in advanced HIV infection. These measurements were then used to evaluate levels of circulating cytokines and chemokines for patterns of relationship to the degree of brain injury. Luminex-determined marker levels were evaluated at a baseline assessment and then again three years later in the course of HIV infection.

At each timepoint, automated brain segmentation algorithms were used to derive volume fractions of gray matter, white matter and cerebrospinal fluid within the individual cranial cavity, as well as the parenchymal volume relative to normative population brain size [8-10]. The derived measurements, which are sensitive to brain atrophy and loss of specific tissue types, have been determined to be robust and accurate in simulation studies against known tissue volumes [8-10]. Segmentation-derived brain volumetric measures have been used to investigate brain changes in HIV infection [11, 12].

Diffusion Tensor Imaging (DTI) was also used to quantify brain status at baseline and at three year follow-up. DTI is based on Brownian motion and statistical principles for the diffusion of protons formalized by Einstein, extended to the interrogation of human brain tissue with Magnetic Resonance [13]. In the usual time scale of the acquisition, water molecules in the brain move measurable distances approximating sizes of cells and sub-cellular structures. Because neuropathological changes systematically alter the microscopic displacement distributions of water molecules, measurements that can be determined with DTI confer information concerning microstructural alterations in the interrogated tissue. Commonly derived DTI measurements include the mean diffusivity (MD), the average diffusion of water molecules in all directions, and the fractional anisotropy (FA), the directionally-dependent diffusion. Owing to its intrinsic organization in directionally aligned fiber tracts, the latter measure, FA, is particularly sensitive to detection of pathological changes in white matter (e.g. to axons). DTI parameters can be calculated for specific regions of interest or across extremely large numbers of volume elements (voxels) to derive

NIH-PA Author Manuscript

NIH-PA Author Manuscript

NIH-PA Author Manuscript

aggregate measures of microstructural injury for the whole brain. DTI measurements have been shown to be sensitive to brain changes occurring in HIV infection and to correlate with dementia [14-18].

2. Materials and Methods

Subjects for this imaging study were recruited from the longitudinal Northeast Aids Dementia (NEAD) cohort study of neurological outcome in HIV infection (8 Males, 2 Females; mean age 47 ± 7.3). Exclusion criteria for this cohort include history of chronic neurological disorders, stroke, head trauma, opportunistic CNS infection or psychosis. The study was conducted with approval of the Institutional Review Board. All subjects signed an informed consent. Blood samples were collected from participants at baseline and at three year follow-up. Seropositivity was confirmed by enzyme-linked immunosorbent assay and Western blot. All subjects were in advanced infection, meeting criteria for AIDS (absolute CD4 cell counts: 24 to 427/mm^3; plasma viral load: undetectable to 154,938 copies/mL) and were on antiretroviral regimens (including protease inhibitors for 9 subjects). Neurological examinations were conducted by a board-certified neurologist and included the Macro-Neurological Examination and the motor portion of the Unified Parkinson's Disease Rating Scale to assess extrapyramidal signs. The Karnofsky Performance Scale was used to assess functional status. The severity of cognitive impairment was evaluated using the Memorial Sloan Kettering (MSK) Staging for HIV associated cognitive impairment [19]. The MSK takes into account CNS abnormalities on examination, impairment in work, self-care, and mobility status reported by the patient, and results of a neuropsychological test battery designed to assess decline in verbal memory, visual memory, constructional skills, psychomotor skills, motor skills, reaction time, frontal systems, and general intellectual performance. A reported deficit in at least one of the eight instrumental activities of daily living is required as minimal functional criterion for MSK staging. The neurological evaluation used in the NEAD study has been described more extensively elsewhere [4, 20, 21]. Table 1 presents clinical information for each patient, including MSK ratings.

Marker levels were quantified at Johns Hopkins in the HIV Neuroscience laboratory using high throughput biological testing, in which a large number of proteins can be analyzed simultaneously. Luminex-based technology uses fluorescent color-coded beads or microspheres coated with assay-specific reagents. The microspheres pass through lasers and high speed digital signal processors to measure the degree of fluorescence. The analyzer reads multiplex assay results by reporting multiple colors on each microsphere particle. Multiplexed assay kits and beads were obtained from Bio-Rad (Hercules, CA). Calibration curves from recombinant cytokine standards were prepared with three-fold dilution steps using the same matrix as the samples. Measurements and data analysis of assays were performed with the Luminex-100 system in combination with Luminex manager software (Bioplex manager, Bio-Rad, Hercules, CA). Each sample was assayed in duplicate on a Bio-Plex 100 Suspension Array Analyzer following standard assay protocols and instructions supplied by the manufacturer. Samples were measured two times, and blank values were subtracted from all readings. The biomarker quality assurance program at the Johns Hopkins HIV Neuroscience Laboratory uses standard operating procedures to review results for unexpected or unacceptable variance (evidence of bead clumping; coefficients of variation greater than 20%; unusual distributions of values; outliers more than 4 standard deviations from the mean). Approximately 85-90% of concentrations meet these guidelines for accurate results at first assay, with repeated assays required in approximately 10-15%. Factors examined in this investigation (measured in pg/mL) included: Eotaxin, granulocyte macrophage colony-stimulating factor (GM-CSF), interferon gamma (IFNγ), interleukins (IL): IL-10, IL-12(p40), IL-12(p70), IL-13, IL-15, IL-1α, IL-1β, IL-2, IL-3, IL-4, IL-5, IL-6, IL-7, IL-8, IP-10, monocyte chemoattractant protein-1 (MCP-1), macrophage inflammatory

NIH-PA Author Manuscript

NIH-PA Author Manuscript

NIH-PA Author Manuscript

protein (MIP-1α), regulated on activation normal T cell expressed and secreted (RANTES) and tumor necrosis factors-α (TNFα).

Neuroradiologic examinations were performed on a 1.5 Tesla twinspeed unit (Milwaukee, USA) with high performance gradients using a quadrature birdcage headcoil for RF transmission and signal reception. T_2- and proton-density-weighted images were acquired using dual spin echo sequences, with repetition time of TR=3300 msec, echo times of TE=20 msec and 90 msec. Other parameters were as follows: flip angle: 90°, matrix size: 256×256, field of view: 24×18 cm, NEX=2, slice thickness/gap: 3.5/0, 42 contiguous slices covering whole brain. DTI was performed with an echo planar sequence and bandwidth of ±125kHz. A b=0 reference image and six diffusion-weighted images with a b-value of 1000sec/mm^2 were acquired at each slice. DTI images were acquired for the entire brain using 22 contiguous 7-mm axial sections (field of view: 24cm, matrix size: 128×128, NEX:4 TR:baseline-7000/followup-6200).

Quantitative image analysis was performed off-line. Image processing algorithms developed at Oxford University were used to determine volumetric measurements (8, 10). The normalized brain parenchyma volume (NBPV), which adjusts for individual differences in brain size, was determined based on T_2-weighted images (8). To calculate volume fractions of gray matter (GM), white matter (WM) and cerebrospinal fluid (CSF), the volume (in mm^3) of each tissue type was divided by total brain volume (as measured by the intracranial cavity), obtained from the T_2- and proton-density weighted MR data (Figure 1). DTI metrics were calculated using customized image-processing routines written in MATLAB (Mathworks, Natick, MA). The background noise was first segmented from tissue by applying an automated thresholding technique to the diffusion-weighted images. This also removed voxels containing predominantly CSF which have low intensity on diffusion-weighted images. Remaining extracranial structures were excluded by manual editing to refine the skull stripping process. Mean diffusivity (MD) and fractional anisotropy (FA) were derived for all remaining voxels, according to standard equations [13]. MD (in units of 10^{-3} mm^2/s) and FA (ranging from 0 to 1) values were calculated across the whole brain (for all non-masked voxels, as described above) and summarized for each subject based on the mean value. Figure 2 presents an FA map at a single slice level and a whole brain FA histogram for an individual subject.

Statistical analyses

Primary variables for analysis included levels for markers within the limits of detection. Quantitative MR measurements included the normalized parenchyma brain volume (NBPV), as well as volume fractions of gray matter (GM), white matter (WM) and cerebrospinal fluid (CSF). The DTI measurements included MD and FA averaged for whole brain as defined above. Distributional assumptions were evaluated for all variables prior to analysis. Relationships between marker levels and MR brain measurements were determined using Pearson correlation coefficients. Analyses were executed with SPSS (Chicago, IL).

3. Results

Means and standard deviations for the MR measurements and cytokine/chemokine levels are presented in Table 2 and the correlations are presented in Tables 3 and 4. Many markers fell uniformly beyond the limits of assay detection in all participants, particularly at baseline (Table 3). More markers were within limits of detection three years later in the clinical course (Table 4). Several were detected in only a subset of the sample (IFNγ and IL-1α at baseline and IFNγ and IL-6 at follow-up).

NIH-PA Author Manuscript

NIH-PA Author Manuscript

NIH-PA Author Manuscript

At the initial baseline assessment, significant correlations were identified between plasma MCP-1 and whole brain fractional anisotropy (r= -0.69; p=0.03). Correlations between MCP-1 and volume fractions of CSF (r=0.55; p=0.10) and GM (r=-0.53; p=0.11) approached significance. No other significant relationships were identified at baseline. At three year follow up (Table 4), significant or nearly significant correlations were identified between concurrent serum MCP-1 and increased CSF (r=0.77; p=0.02), reduced GM fraction (r= -0.83; p=0.004) and reduced normalized parenchymal brain volume (r=-.64; p=.06). MCP-1 was also significantly correlated with both DTI measurements: increased MD (r=0.66; p=.05) and reduced FA (r= -0.63; p=0.05). Finally, at follow-up several other analytes demonstrated significant or nearly significant correlations with WM volume fraction, including eotaxin (r= -0.66; p=0.05); granulocyte macrophage colony-stimulating factor (r=-0.62; p=0.07), IL-4 (r=-0.60; p=0.07) and RANTES (r=-0.77; p=0.07). A correlation between normalized parenchymal brain volume and IL-7 (r=0.83; p=0.04) was also observed at follow-up.

4. Discussion

Of the markers examined, MCP-1 (Monocyte Chemoattractant Protein-1 or CCL-2) was the most prominent correlate of brain injury in individuals in advanced HIV infection. At baseline, elevated MCP-1 levels correlated with reduced anisotropy, a DTI measure reflecting loss of white matter integrity from destruction or disruption of axons. Demyelination, sublethal injury or displacement of axonal fibers with less ordered cells, such as multinucleated giant cells (the HIV-D pathologic hallmark), will reduce the directional diffusion, or FA. HIV-Encephalitis, the pathological correlate of dementia, involves heterogeneous inflammatory and degenerative changes. Whole brain DTI parameters, such as FA, afford measures of aggregate microstructural changes in brain tissue. Of the studied MR measures, FA may be the most sensitive to sublethal, microstructural brain changes.

The relationship of plasma MCP-1 to brain injury was more extensive three years later. Follow-up MCP-1 levels correlated with both whole brain DTI measurements, including reduced anisotropy, replicating the baseline findings, and with increased mean diffusivity. Membranes, membrane permeability and the relative volume and morphology of the extracellular space are determinants of MD [22]. The relationship of MCP-1 with increased MD is consistent with neuronal loss, or secondary destruction of white matter fibers due to neuronal death, loss of structural barriers and expansion of the extracellular space. At follow-up, MCP-1 levels also demonstrated a marked relationship to brain volumetric measurements derived with segmentation, including reduced gray matter and increased CSF volume fractions, and with brain parenchyma volume relative to normative population brain size. These findings are also consistent with irreversible neuronal loss and brain atrophy, a common finding in autopsy and imaging studies of HIV-Dementia [1]. The relationship with increased CSF reflects such changes as the widened sulcus filled with CSF corresponding to shrinkage of cortical gray matter and enlargement of ventricles associated with shrinkage of subcortical brain tissue. MCP-1 has also been implicated in neurodegeneration in other disorders [23-25], including multiplexed findings in Alzheimer’s Disease [26].

These findings add to evidence of MCP-1 involvement in HIV brain injury and associated cognitive deterioration [27]. MCP-1 levels predict cognitive deterioration [4] as well as encephalitis in animal models [28, 29]. Plasma MCP-1 levels correlate with diffusion abnormalities in basal ganglia and deep white matter, regions that are vulnerable to injury in infected individuals [30]. MCP-1 levels are elevated in brain tissue and CSF in association with HIV-Dementia [31] and HIV-Encephalitis [32]. Elevated CSF MCP-1 levels correlate with microvascular changes and blood brain barrier impairment determined by MR

NIH-PA Author Manuscript

NIH-PA Author Manuscript

NIH-PA Author Manuscript

perfusion [33], with glial metabolites [34, 35] and, among untreated subjects, with neuronal dysfunction/loss determined by MR spectroscopy [35].

Escalation in trafficking of activated monocytes into the brain may be a critical determinant of dementia in HIV infection [36]. MCP-1 is a potent monocyte chemoattractant that enhances both trafficking and ingress of these cells into the brain [37-42]. Levels of activated monocytes (macrophage precursors) in the circulation, as well as the extent of activated macrophages in brain tissue [43], correlate with dementia. HIV is imported into the brain via blood-borne monocytes (macrophage precursors). Monocytes entering the brain activate uninfected macrophages and resident microglia and as this escalates, vicious cycles of macrophage dysregulation may ensue [36]. CNS production of proinflammatory cytokines, chemokines and neurotoxic viral gene products may lead to extensive brain injury [44]. MCP-1 may influence viral replication within the brain [45], which occurs primarily in cells of monocytic lineage (monocyte-derived macrophages and microglia), alter the inflammatory cascade [46] or otherwise interact with viral proteins [38, 47-52]. Experimental evidence suggests that MCP-1 primes the responsiveness of glia to inflammatory stimuli [53] and an MCP-1 antagonist delays onset and reduces neurological signs associated with neuroinflammation [54]. Both MCP-1 levels (plasma and CSF) and symptomatic neurological progression have been identified as predictors of death in HIV infection (e.g. [3, 20].

A polymorphism MCP-1 allele has been linked to high levels of MCP-1, accelerated systemic HIV disease progression and markedly increased risk of dementia [55]. Some individuals may mount more exaggerated responses to infection and secrete higher levels of cytokines/chemokines across the clinical course. Serial plasma studies from pre-infection to seroconversion indicate marked individual differences in induction of plasma cytokines and chemokines during exponential viral amplification of acute HIV[56]. All subjects in this small intensive study were in advanced infection (AIDS). Factors serving neuroprotection or repair may become neurotoxic under excessive or chronic upregulation [57]. Some experimental evidence, for example, suggests that MCP-1 may allay neuronal and astrocyte apoptosis by the neurotoxic HIV viral protein, *tat* [58]. Given the dynamic nature of immune mediators, the prognostic significance of a specific marker may change across infection, depending on whether relevant disease activity is active or quiescent, the degree of immunosuppression or other factors.

In this investigation, some markers fell uniformly beyond limits of assay detection in all participants, particularly at baseline (Table 2). Several markers (IFNγ and IL-1α at baseline and IFNγ and IL-6 at follow-up) were detected only in a subset of participants. Other MR/marker relationships were noted: for white matter volume (e.g. eotaxin, GM-CSF, IL-4 and RANTES) and for brain volume (IL-7). Findings for these analytes require further replication. The limited number of subjects does not allow definitive conclusions regarding all markers analyzed here. The neuropathophysiologic significance of MCP-1, however, is supported by the consistent pattern of findings with multiple MR brain status measurements at two separate timepoints across three years of infection.

Concluding remarks. Determination of factors underlying variability in HIV neurological outcome is imperative for preservation of the brain and cognitive function. Studies using proteomic profiling have uncovered new markers of interest for further study [59-62]. This investigation demonstrates the synergistic potential of multiplexed analysis used together with quantitative brain imaging strategies for evaluating markers. This approach enhances efficiency of marker screening with smaller sample sizes. The automated image analysis tools used in this investigation require minimal operator input and can also be adapted to large-scale investigations to illuminate meaningful interactions between markers of interest.

NIH-PA Author Manuscript

NIH-PA Author Manuscript

NIH-PA Author Manuscript

Multiple factors are likely to be associated with, or predictive of neurological progression in HIV infection. Proteomic applications promise to accelerate identification of risk and protective markers associated with individual differences in susceptibility, progression and clinical outcome in HIV infection and other CNS disorders.

Acknowledgments

Funding: This work was supported by National Institutes of Health [grant numbers MH66705, MH080636, MH075673, NS044807(JCM) and NS049465(JCM)].

References

1. McArthur JC, Brew BJ, Nath A. Neurological complications of HIV infection. Lancet Neurol. 2005; 4:543–555. [PubMed: 16109361]
2. Antinori A, Arendt G, Becker JT, Brew BJ, et al. Updated research nosology for HIV-associated neurocognitive disorders. Neurology. 2007; 69:1789–1799. [PubMed: 17914061]
3. Tozzi V, Balestra P, Lorenzini P, Bellagamba R, et al. Prevalence and risk factors for human immunodeficiency virus-associated neurocognitive impairment, 1996 to 2002: results from an urban observational cohort. Journal of neurovirology. 2005; 11:265–273. [PubMed: 16036806]
4. Sevigny JJ, Albert SM, McDermott MP, McArthur JC, et al. Evaluation of HIV RNA and markers of immune activation as predictors of HIV-associated dementia. Neurology. 2004; 63:2084–2090. [PubMed: 15596754]
5. Cherner M, Cysique L, Heaton RK, Marcotte TD, et al. Neuropathologic confirmation of definitional criteria for human immunodeficiency virus-associated neurocognitive disorders. Journal of neurovirology. 2007; 13:23–28. [PubMed: 17454445]
6. Thurnher MM, Donovan Post MJ. Neuroimaging in the brain in HIV-1-infected patients. Neuroimaging clinics of North America. 2008; 18:93–117. viii. [PubMed: 18319157]
7. Price RW, Epstein LG, Becker JT, Cinque P, et al. Biomarkers of HIV-1 CNS infection and injury. Neurology. 2007; 69:1781–1788. [PubMed: 17967994]
8. Smith SM, Zhang Y, Jenkinson M, Chen J, et al. Accurate, robust, and automated longitudinal and cross-sectional brain change analysis. Neuroimage. 2002; 17:479–489. [PubMed: 12482100]
9. Smith SM, Jenkinson M, Woolrich MW, Beckmann CF, et al. Advances in functional and structural MR image analysis and implementation as FSL. Neuroimage. 2004; 23(Suppl 1):S208–219. [PubMed: 15501092]
10. Zhang Y, Brady M, Smith S. Segmentation of brain MR images through a hidden Markov random field model and the expectation-maximization algorithm. IEEE Transactions on Medical Imaging. 2001; 20:45–57. [PubMed: 11293691]
11. Thompson P, Dutton R, Hayashi K, Allen L, et al. 3D mapping of ventricular and corpus callosum abnormalities in HIV/AIDS. NeuroImage. 2005
12. Thompson PM, Dutton RA, Hayashi KM, Toga AW, et al. Thinning of the cerebral cortex visualized in HIV/AIDS reflects CD4+ T lymphocyte decline. Proceedings of the National Academy of Sciences of the United States of America. 2005; 102:15647–15652. [PubMed: 16227428]
13. Basser PJ, Pierpaoli C. Microstructural and physiological features of tissues elucidated by quantitative-diffusion-tensor MRI. J Magn Reson B. 1996; 111:209–219. [PubMed: 8661285]
14. Filippi CG, Ulug AM, Ryan E, Ferrando SJ, van Gorp W. Diffusion tensor imaging of patients with HIV and normal-appearing white matter on MR images of the brain. Ajnr. 2001; 22:277–283. [PubMed: 11156769]
15. Pomara N, Crandall DT, Choi SJ, Johnson G, Lim KO. White matter abnormalities in HIV-1 infection: a diffusion tensor imaging study. Psychiatry Res. 2001; 106:15–24. [PubMed: 11231096]
16. Ragin AB, Storey P, Cohen BA, Edelman RR, Epstein LG. Disease burden in HIV-associated cognitive impairment: a study of whole-brain imaging measures. Neurology. 2004; 63:2293–2297. [PubMed: 15623689]

NIH-PA Author Manuscript

NIH-PA Author Manuscript

NIH-PA Author Manuscript

17. Pfefferbaum A, Rosenbloom MJ, Adalsteinsson E, Sullivan EV. Diffusion tensor imaging with quantitative fibre tracking in HIV infection and alcoholism comorbidity: synergistic white matter damage. Brain. 2007; 130:48–64. [PubMed: 16959813]
18. Thurnher MM, Castillo M, Stadler A, Rieger A, et al. Diffusion-tensor MR imaging of the brain in human immunodeficiency virus-positive patients. Ajnr. 2005; 26:2275–2281. [PubMed: 16219833]
19. Price RW, Brew BJ. The AIDS dementia complex. Journal of Infectious Diseases. 1988; 158:1079–1083. [PubMed: 3053922]
20. Sevigny JJ, Albert SM, McDermott MP, Schifitto G, et al. An evaluation of neurocognitive status and markers of immune activation as predictors of time to death in advanced HIV infection. Arch Neurol. 2007; 64:97–102. [PubMed: 17210815]
21. Wachtman LM, Skolasky RL, Tarwater PM, Esposito D, et al. Platelet decline: an avenue for investigation into the pathogenesis of human immunodeficiency virus -associated dementia. Arch Neurol. 2007; 64:1264–1272. [PubMed: 17846264]
22. Le Bihan D. Looking into the functional architecture of the brain with diffusion MRI. Nature reviews. 2003; 4:469–480.
23. Losy J, Zaremba J. Monocyte chemoattractant protein-1 is increased in the cerebrospinal fluid of patients with ischemic stroke. Stroke; a journal of cerebral circulation. 2001; 32:2695–2696.
24. Henkel JS, Beers DR, Siklos L, Appel SH. The chemokine MCP-1 and the dendritic and myeloid cells it attracts are increased in the mSOD1 mouse model of ALS. Molecular and cellular neurosciences. 2006; 31:427–437. [PubMed: 16337133]
25. Galimberti D, Schoonenboom N, Scarpini E, Scheltens P. Chemokines in serum and cerebrospinal fluid of Alzheimer's disease patients. Annals of neurology. 2003; 53:547–548. [PubMed: 12666129]
26. Sokolova A, Hill MD, Rahimi F, Warden LA, et al. Monocyte Chemoattractant Protein-1 Plays a Dominant Role in the Chronic Inflammation Observed in Alzheimer's Disease. Brain pathology (Zurich, Switzerland). 2008
27. Dhillon NK, Williams R, Callen S, Zien C, et al. Roles of MCP-1 in development of HIV-dementia. Front Biosci. 2008; 13:3913–3918. [PubMed: 18508485]
28. Zink MC, Coleman GD, Mankowski JL, Adams RJ, et al. Increased macrophage chemoattractant protein-1 in cerebrospinal fluid precedes and predicts simian immunodeficiency virus encephalitis. Journal of Infectious Diseases. 2001; 184:1015–1021. erratum appears in J Infect Dis 2002 Jun 1;185(11):1696. [PubMed: 11574916]
29. Mankowski JL, Queen SE, Clements JE, Zink MC. Cerebrospinal fluid markers that predict SIV CNS disease. Journal of neuroimmunology. 2004; 157:66–70. [PubMed: 15579282]
30. Ragin AB, Wu Y, Storey P, Cohen BA, et al. Monocyte chemoattractant protein-1 correlates with subcortical brain injury in HIV infection. Neurology. 2006; 66:1255–1257. [PubMed: 16636247]
31. Kelder W, McArthur JC, Nance-Sproson T, McClernon D, Griffin DE. Beta-chemokines MCP-1 and RANTES are selectively increased in cerebrospinal fluid of patients with human immunodeficiency virus-associated dementia. Annals of neurology. 1998; 44:831–835. [PubMed: 9818943]
32. Cinque P, Vago L, Mengozzi M, Torri V, et al. Elevated cerebrospinal fluid levels of monocyte chemotactic protein-1 correlate with HIV-1 encephalitis and local viral replication. AIDS (London, England). 1998; 12:1327–1332.
33. Avison MJ, Nath A, Greene-Avison R, Schmitt FA, et al. Inflammatory changes and breakdown of microvascular integrity in early human immunodeficiency virus dementia. Journal of neurovirology. 2004; 10:223–232. [PubMed: 15371152]
34. Avison MJ, Nath A, Greene-Avison R, Schmitt FA, et al. Neuroimaging correlates of HIV-associated BBB compromise. Journal of neuroimmunology. 2004; 157:140–146. [PubMed: 15579291]
35. Chang L, Ernst T, St Hillaire C, Conant K. Antiretroviral treatment alters relationship between MCP-1 and neurometabolites in HIV patients. Antivir Ther. 2004; 9:431–440. [PubMed: 15259906]
36. Gartner S. HIV infection and dementia. Science. 2000; 287:602–604. [PubMed: 10691542]

NIH-PA Author Manuscript

NIH-PA Author Manuscript

NIH-PA Author Manuscript

37. Conant K, McArthur JC, Griffin DE, Sjulson L, et al. Cerebrospinal fluid levels of MMP-2, 7, and 9 are elevated in association with human immunodeficiency virus dementia. Annals of Neurology. 1999; 46:391–398. [PubMed: 10482270]
38. Weiss JM, Nath A, Major EO, Berman JW. HIV-1 Tat induces monocyte chemoattractant protein-1-mediated monocyte transmigration across a model of the human blood-brain barrier and upregulates CCR5 expression on human monocytes. Journal of Immunology. 1999; 163:2953–2959.
39. Langford D, Masliah E. Crosstalk between components of the blood brain barrier and cells of the CNS in microglial activation in AIDS. Brain pathology (Zurich, Switzerland). 2001; 11:306–312.
40. Persidsky Y, Ghorpade A, Rasmussen J, Limoges J, et al. Microglial and astrocyte chemokines regulate monocyte migration through the blood-brain barrier in human immunodeficiency virus-1 encephalitis. The American journal of pathology. 1999; 155:1599–1611. [PubMed: 10550317]
41. Persidsky Y, Zheng J, Miller D, Gendelman HE. Mononuclear phagocytes mediate blood-brain barrier compromise and neuronal injury during HIV-1-associated dementia. Journal of leukocyte biology. 2000; 68:413–422. [PubMed: 10985259]
42. Sasseville VG, Newman W, Brodie SJ, Hesterberg P, et al. Monocyte adhesion to endothelium in simian immunodeficiency virus-induced AIDS encephalitis is mediated by vascular cell adhesion molecule-1/alpha 4 beta 1 integrin interactions. American Journal of Pathology. 1994; 144:27–40. [PubMed: 7507300]
43. Glass JD, Fedor H, Wesselingh SL, McArthur JC. Immunocytochemical quantitation of human immunodeficiency virus in the brain: correlations with dementia. Annals of neurology. 1995; 38:755–762. [PubMed: 7486867]
44. Williams KC, Hickey WF. Central nervous system damage, monocytes and macrophages, and neurological disorders in AIDS. Annual Review of Neuroscience. 2002; 25:537–562.
45. Williams K, Alvarez X, Lackner AA. Central nervous system perivascular cells are immunoregulatory cells that connect the CNS with the peripheral immune system. Glia. 2001; 36:156–164. [PubMed: 11596124]
46. Ferreira AM, Rollins BJ, Faunce DE, Burns AL, et al. The effect of MCP-1 depletion on chemokine and chemokine-related gene expression: evidence for a complex network in acute inflammation. Cytokine. 2005; 30:64–71. [PubMed: 15804597]
47. Eugenin EA, Dyer G, Calderon TM, Berman JW. HIV-1 tat protein induces a migratory phenotype in human fetal microglia by a CCL2 (MCP-1)-dependent mechanism: possible role in NeuroAIDS. Glia. 2005; 49:501–510. [PubMed: 15578658]
48. Lehmann MH, Masanetz S, Kramer S, Erfle V. HIV-1 Nef upregulates CCL2/MCP-1 expression in astrocytes in a myristoylation- and calmodulin-dependent manner. Journal of cell science. 2006; 119:4520–4530. [PubMed: 17046994]
49. Albini A, Ferrini S, Benelli R, Sforzini S, et al. HIV-1 Tat protein mimicry of chemokines. Proc Natl Acad Sci U S A. 1998; 95:13153–13158. [PubMed: 9789057]
50. McManus CM, Weidenheim K, Woodman SE, Nunez J, et al. Chemokine and chemokine-receptor expression in human glial elements: induction by the HIV protein, Tat, and chemokine autoregulation. The American journal of pathology. 2000; 156:1441–1453. [PubMed: 10751368]
51. D'Aversa TG, Yu KO, Berman JW. Expression of chemokines by human fetal microglia after treatment with the human immunodeficiency virus type 1 protein Tat. Journal of neurovirology. 2004; 10:86–97. [PubMed: 15204927]
52. Eldeen MB, Deshmane SL, Simbiri K, Khalili K, et al. MH2 domain of Smad3 reduces HIV-1 Tat-induction of cytokine secretion. Journal of neuroimmunology. 2006; 176:174–180. [PubMed: 16750572]
53. Rankine EL, Hughes PM, Botham MS, Perry VH, Felton LM. Brain cytokine synthesis induced by an intraparenchymal injection of LPS is reduced in MCP-1-deficient mice prior to leucocyte recruitment. The European journal of neuroscience. 2006; 24:77–86. [PubMed: 16882009]
54. Buntinx M, Hermans B, Goossens J, Moechars D, et al. Pharmacological profile of JNJ-27141491 [(S)-3-[3,4-difluorophenyl)-propyl]-5-isoxazol-5-yl-2-thioxo-2,3-dihydro-1 H-imidazole-4-carboxyl acid methyl ester], as a noncompetitive and orally active antagonist of the human

NIH-PA Author Manuscript

NIH-PA Author Manuscript

NIH-PA Author Manuscript

chemokine receptor CCR2. The Journal of pharmacology and experimental therapeutics. 2008; 327:1–9. [PubMed: 18599682]

55. Gonzalez E, Rovin BH, Sen L, Cooke G, et al. HIV-1 infection and AIDS dementia are influenced by a mutant MCP-1 allele linked to increased monocyte infiltration of tissues and MCP-1 levels. Proc Natl Acad Sci U S A. 2002; 99:13795–13800. [PubMed: 12374865]
56. Stacey AR, Norris PJ, Qin L, Haygreen EA, et al. induction of a striking systemic cytokine cascade prior to peak viremia in acute human immunodeficiency virus type 1 infection, in contrast to more modest and delayed responses in acute hepatitis B and C virus infections. J Virol. 2009; 83:3719–3733. [PubMed: 19176632]
57. Brew BJ. Lost in translation: again, another failed neuroprotection trial. Neurology. 2007; 69:1308–1309. [PubMed: 17893290]
58. Eugenin EA, D'Aversa TG, Lopez L, Calderon TM, Berman JW. MCP-1 (CCL2) protects human neurons and astrocytes from NMDA or HIV-tat-induced apoptosis. Journal of neurochemistry. 2003; 85:1299–1311. [PubMed: 12753088]
59. Wojna V, Carlson KA, Luo X, Mayo R, et al. Proteomic fingerprinting of human immunodeficiency virus type 1-associated dementia from patient monocyte-derived macrophages: A case study. Journal of neurovirology. 2004; 10(Suppl 1):74–81. [PubMed: 14982743]
60. Berger JR, Avison M, Mootoor Y, Beach C. Cerebrospinal fluid proteomics and human immunodeficiency virus dementia: preliminary observations. Journal of neurovirology. 2005; 11:557–562. [PubMed: 16338749]
61. Laspiur JP, Anderson ER, Ciborowski P, Wojna V, et al. CSF proteomic fingerprints for HIV-associated cognitive impairment. Journal of neuroimmunology. 2007; 192:157–170. [PubMed: 17950469]
62. Rozek W, Ricardo-Dukelow M, Holloway S, Gendelman HE, et al. Cerebrospinal fluid proteomic profiling of HIV-1-infected patients with cognitive impairment. Journal of proteome research. 2007; 6:4189–4199. [PubMed: 17929958]

List of Abbreviations

AIDS	acquired immune deficiency syndrome
CSF	cerebrospinal fluid
DTI	Diffusion Tensor Imaging
FA	fractional anisotropy
GM	gray matter
GM-CSF	granulocyte macrophage colony-stimulating factor
HAND	HIV-associated neurocognitive disorder
HIV	Human Immunodeficiency Virus
HIV RNA	viral replication measured in the peripheral circulation
IFNγ	interferon gamma
IL	Interleukin
IP-10	Interferon inducible protein 10
MCP-1 (also CCL-2)	Monocyte Chemoattractant Protein 1
MD	mean diffusivity
MIP-1α:	macrophage inflammatory protein
MR	Magnetic Resonance
MSK	Memorial Sloan Kettering dementia rating scale

NIH-PA Author Manuscript

NIH-PA Author Manuscript

NIH-PA Author Manuscript

NBPV	normalized parenchymal brain volume
RANTES	regulated on activation normal T cell expressed and secreted 3D: three dimensional
TNFα	tumor necrosis factors-α
WM	white matter

NIH-PA Author Manuscript

NIH-PA Author Manuscript

NIH-PA Author Manuscript

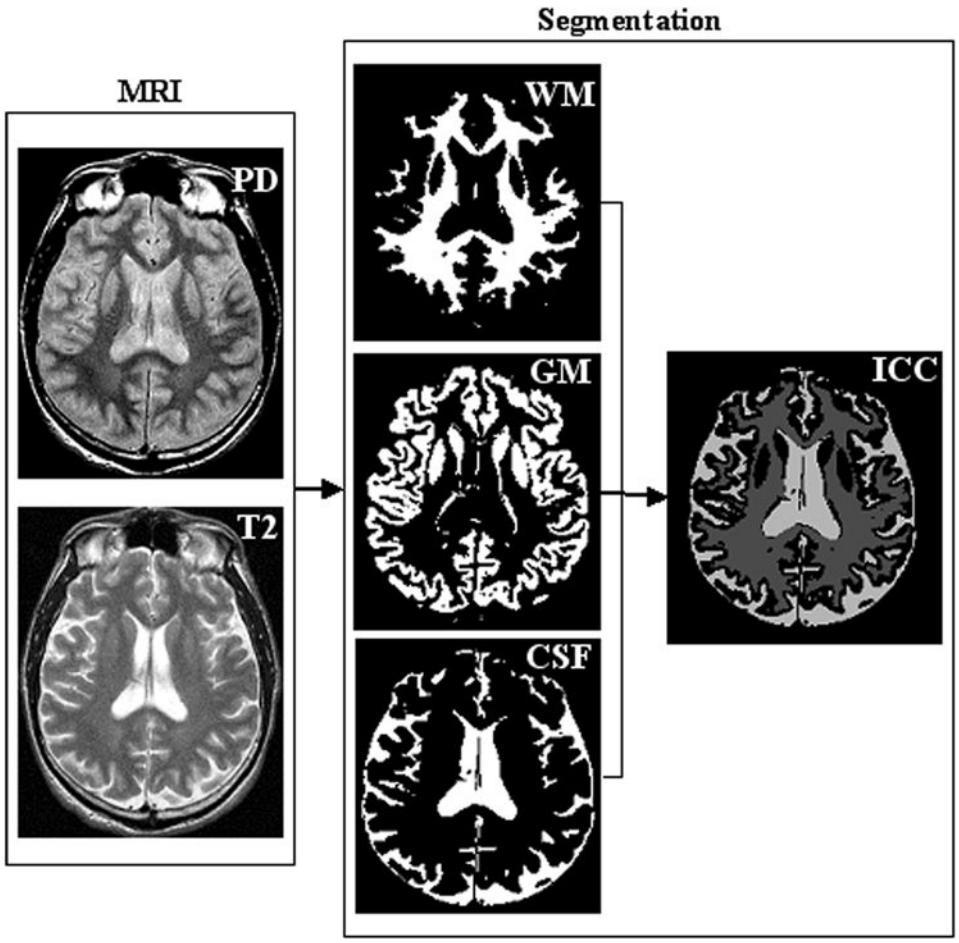

FIGURE 1. AUTOMATED BRAIN SEGMENTATION

BRAIN ATROPHY CAN BE SEEN ON CONVENTIONAL MR IMAGES OF HIV INFECTED PATIENTS. IT IS DIFFICULT TO DETERMINE OF INJURY BASED ON VISUAL INSPECTION. AUTOMATED IMAGE PROCESSING ALGORITHMS CAN BE USED TO QUANTIFY THE BRAIN PARENCHYMA FRACTION, RELATIVE TO NORMATIVE POPULATION VALUES. VOLUME FRACTIONS OF GRAY MATTER, WHITE MATTER AND CSF CAN BE DETERMINED FOR EACH SUBJECT RELATIVE TO THE INDIVIDUAL INTRACRANIAL CAVITY (ICC) VOLUME (RIGHT). THESE ALGORITHMS REQUIRE MINIMAL OPERATOR, THEREBY MINIMIZING INTER- AND INTRA-RATER VARIATION IN BRAIN VOLUMETRIC MEASUREMENT.

NIH-PA Author Manuscript

NIH-PA Author Manuscript

NIH-PA Author Manuscript

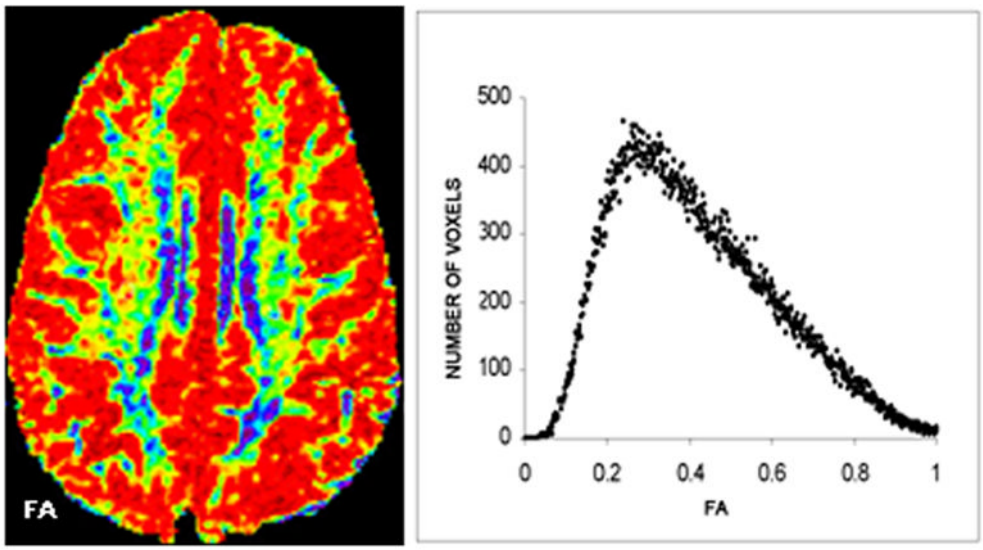

FIGURE 2.

LEFT: A FRACTIONAL ANISOTROPY (FA) MAP AT A SINGLE SLICE, COLORIZED TO ILLUSTRATE VARIABILITY IN VALUES (RED LOWEST; BLUE HIGHEST). RIGHT: WHOLE BRAIN DISTRIBUTION OF FA VALUES (RANGING FROM 0 to 1), SHOWN FOR AN INDIVIDUAL SUBJECT IN A HISTOGRAM. THE MEAN WAS USED TO SUMMARIZE “WHOLE BRAIN” FA. DIFFUSION MAPS CAN ALSO BE USED TO CALCULATE MEAN DIFFUSIVITY (MD).

NIH-PA Author Manuscript NIH-PA Author Manuscript NIH-PA Author Manuscript

Table 1

Clinical Characteristics

	Baseline								3 Year Follow-up								
Subject	**Age**	**CD4**	**Viral Load**	**CD8**	**BMI**	**Hemoglobin**	**MSK**	**KPS**	**CD4**	**Nadir CD4***	**Viral Load**	**Avg Viral Load***	**CD8**	**BMI**	**Hemoglobin**	**MSK**	**KPS**
1	62	220	87	420	24.9	13.7	1	90	294	191	< 50	57	525	24.4	13.4	0.5	90
2	42	108	172	803	23.8	13.9	1	60	367	108	152	756	1056	21.9	13.3	1	60
3	49	397	<50	1021	21.2	12.7	1	65	777	13	< 50	77494	1018	24.3	12.4	2	70
4	59	81	3927	1048	23.7	13.4	0.5	80	74	10	351	1015	684	21.4	13.5	1	80
5	38	373	< 50	1664	23.7	15.2	0.5	100	737	176	< 50	< 50	1536	27.7	15.0	0	100
6	54	427	< 50	1708	18.4	14.4	0.5	90	649	119	< 50	1853	1766	18.0	15.7	0	70
7	52	310	< 50	1336	28.7	13.0	0.5	100	350	187	< 50	10245	1213	32.9	14.0	0	100
8	42	24	154938	324	27.6	11.0	0.5	80	50	24	55300	57440	462	31.6	14.8	1	60
9	48	122	20611	1486	24.0	13.3	1	75	199	61	< 50	51963	1176	27.7	13.3	1	70
10	49	340	2718	1339	20.8	13.8	0.5	90	303	122	< 50	11665	794	20.2	14.2	0	90

BMI: Body Mass Index. MSK: Memorial Sloan Kettering Dementia Scale. KPS: Karnofsky Performance Scale.

*Based, on available clinical information for an average of 5 prior years.

NIH-PA Author Manuscript
NIH-PA Author Manuscript
NIH-PA Author Manuscript

Table 2

Means and Standard Deviations for MR and Marker Measures

Measure	Baseline		3 Year Follow-up	
NBPV	.79	(.02)	.79	(.03)
GM fraction	.38	(.02)	.39	(.03)
WM fraction	.31	(.02)	.30	(.02)
CSF fraction	.19	(.02)	.19	(.03)
DTI: MD	1.02	(.06)	1.01	(.07)
DTI: FA	.26	(.01)	.24	(.01)
Eotaxin	53.44	(38.30)	132.67	(74.43)
GM-CSF	---	---	21.72	(11.80)
IFNγ	51.82	(30.97)	38.11	(19.75)
IL-10	---	---	---	---
IL-12p40	148.40	(24.20)	362.89	(61.35)
IL-12P70	---	---	---	---
IL-13	---	---	---	---
IL-15	---	---	11.45	(4.98)
IL-1α	151.74	(74.81)	97.20	(32.70)
IL-1β	---	---	---	---
IL-2	---	---	34.69	(7.17)
IL-3	---	---	68.12	(13.52)
IL-4	---	---	10.10	(13.64)
IL-5	---	---	---	---
IL-6	---	---	25.00	(17.80)
IL-7	---	---	14.09	(4.94)
IL-8	23.50	(17.21)	52.93	(11.89)
IP-10	129.22	(58.61)	259.89	(31.17)
MCP-1	54.52	(28.00)	132.47	(46.84)
MIP-1α	180.77	(85.95)	161.56	(55.65)
RANTES	1000.60	(334.28)	5352.88	(3410.66)
TNFα	---	---	109.89	(53.12)

Abbreviations: NBPV:normalized parenchymal brain volume, WM: white matter, GM: gray matter, CSF: cerebrospinal fluid, MD: mean diffusivity, FA: fractional anisotropy.

---Beyond limits of assay detection (uniformly low) in all subjects. Markers in pg/mL.

NIH-PA Author Manuscript NIH-PA Author Manuscript NIH-PA Author Manuscript

Proteomics Clin Appl. Author manuscript; available in PMC 2011 December 20.

Table 3

Correlations between Markers and Brain Status at Baseline

MARKER	NBPV	WM	GM	CSF	MD	FA
Eotaxin	-.24	-.06	-.48	.30	-.38	-.54
GM-CSF	---	---	---	---	---	---
IFNγ	†	†	†	†	†	†
IL-10	---	---	---	---	---	---
IL-12p40	.12	.02	-.02	-.12	-.23	-.06
IL-12P70	---	---	---	---	---	---
IL-13	---	---	---	---	---	---
IL-15	---	---	---	---	---	---
IL-1α	†	†	†	†	†	†
IL-1β	---	---	---	---	---	---
IL-2	---	---	---	---	---	---
IL-3	---	---	---	---	---	---
IL-4	---	---	---	---	---	---
IL-5	---	---	---	---	---	---
IL-6	---	---	---	---	---	---
IL-7	---	---	---	---	---	---
IL-8	-.05	-.12	-.20	.230	-.20	-.23
IP-10	-.31	-.15	-.44	.31	.30	-.27
MCP-1	-.49	-.24	-.53	.55(*)	-.23	-.69*
MIP-1α	.02	-.09	-.27	.14	-.34	-.14
RANTES	.27	.11	.52	-.42	.01	.30
TNFα	---	---	---	---	---	---

Abbreviations: NBPV:normalized parenchymal brain volume, WM: white matter, GM: gray matter, CSF: cerebrospinal fluid, MD: mean diffusivity, FA: fractional anisotropy.

† Beyond limits of detection (low) in at least half of the subjects.

--- Beyond limits of assay detection (uniformly low) in all subjects.

* $p < .05$;

(*) $p < .10$

NIH-PA Author Manuscript NIH-PA Author Manuscript NIH-PA Author Manuscript

Table 4

Correlations between Markers & Brain Status at 3 Yr Follow-Up

Marker	NBPV	WM	GM	CSF	MD	FA
Eotaxin	-.14	-.66*	-.10	.29	.37	-.55
GM-CSF	.26	-.62(*)	.24	-.07	-.13	-.40
IFNγ	.42	-.42	.42	-.32	-.32	-.17
IL-10	---	---	---	---	---	---
IL-12p40	.28	-.04	.00	-.12	-.28	-.08
IL-12P70	---	---	---	---	---	---
IL-13	---	---	---	---	---	---
IL-15	.34	-.47	.44	-.20	-.31	-.26
IL-1α	†	†	†	†	†	†
IL-1β	---	---	---	---	---	---
IL-2	.41	-.51	.46	-.26	-.24	-.29
IL-3	.23	-.20	.02	-.08	-.08	-.30
IL-4	.36	-.60(*)	.46	-.26	-.20	-.34
IL-5	---	---	---	---	---	---
IL-6	†	†	†	†	†	†
IL-7	.83*	-.15	.48	-.64	-.51	.12
IL-8	.24	-.37	.07	.02	-.17	-.31
IP-10	.05	-.20	-.01	.09	-.17	-.03
MCP-1	-.64*	-.24	-.83**	.77**	.66*	-.63*
MIP-1α	.52	-.36	.40	-.36	-.36	-.17
RANTES	-.36	-.44	-.06	.32	.24	-.44
TNFα	.09	-.42	.25	-.06	-.08	-.40

Abbreviations: NBPV:normalized parenchymal brain volume, WM: white matter, GM: gray matter, CSF: cerebrospinal fluid, MD: mean diffusivity, FA: fractional anisotropy.

† Beyond limits of detection (low) in at least half of the subjects.

--- Beyond limits of assay detection (uniformly low) in all subjects.

* $p < .05$;

** p.01; (*) p<.10

NIH-PA Author Manuscript

NIH-PA Author Manuscript

NIH-PA Author Manuscript